Electric field and temperature effects on water in the narrow nonpolar pores of carbon nanotubes

Subramanian Vaitheeswaran[a)]
Laboratory of Chemical Physics, National Institute of Diabetes and Digestive and Kidney Diseases, National Institutes of Health, Building 5, Bethesda, Maryland 20892-0520 and Department of Physics and Astronomy, University of Maine, Orono, Maine 04469

Jayendran C. Rasaiah[b)]
Department of Chemistry, University of Maine, Orono, Maine 04469

Gerhard Hummer[c)]
Laboratory of Chemical Physics, National Institute of Diabetes and Digestive and Kidney Diseases, National Institutes of Health, Building 5, Bethesda, Maryland 20892-0520

(Received 22 April 2004; accepted 29 July 2004)

Water molecules in the narrow cylindrical pore of a (6,6) carbon nanotube form single-file chains with their dipoles collectively oriented either up or down along the tube axis. We study the interaction of such water chains with homogeneous electric fields for finite closed and infinite periodically replicated tubes. By evaluating the grand-canonical partition function term-by-term, we show that homogeneous electric fields favor the filling of previously empty nanotubes with water from the bulk phase. A two-state description of the collective water dipole orientation in the nanotube provides an excellent approximation for the dependence of the water-chain polarization and the filling equilibrium on the electric field. The energy and entropy contributions to the free energy of filling the nanotube were determined from the temperature dependence of the occupancy probabilities. We find that the energy of transfer depends sensitively on the water-tube interaction potential, and that the entropy of one-dimensionally ordered water chains is comparable to that of bulk water. We also discuss implications for proton transfer reactions in biology. © *2004 American Institute of Physics.* [DOI: 10.1063/1.1796271]

I. INTRODUCTION

Low-dimensional confinement can induce ordering,[1] as seen in the formation of ionic nanocrystals[2,3] and hydrogen-bonded water chains inside water nanotubes.[4] For water, wetting behavior[5] and filling of the nanotube interior is highly sensitive to the strength of the interactions between water molecules and the nanotube,[4,6] or, equivalently, changes in the solvent conditions (such as osmolality, temperature, pressure, etc.). Similar effects were seen, e.g., for water between nonpolar plates[7,8] and in hydrophobic pores through membrane models,[9–11] in lattice-gas models of hydrophobic channels,[12,13] and in closed spherical[14,15] and infinite cylindrical pores.[16] A substantial barrier can exist between the filled and empty state of the tube, caused by the energetic cost of fragmenting the hydrogen-bond chain in a partially filled tube. This can result in two statelike fluctuations between filled and empty states.[4,6] Such filling and emptying transitions of hydrophobic pores may be relevant for gating in biological channels.[4,9–11,17,18]

The dipole moments of water molecules in the quasi one-dimensional hydrogen-bonded chains inside the filled nanotube are strongly and collectively oriented, either pointing ''up'' or ''down'' along the tube axis (Fig. 1). This has important implications on the transport of protons through such chains via a Grotthuss-type hopping mechanism.[19–21] For such chains, fast proton diffusion coefficients have been determined in simulations,[20,21] exceeding those in bulk water by a factor of 40 if corrected for the coupling to a hydrogen-bonding defect in a periodically replicated water chain with an excess proton.[21]

The collective dipolar orientations of single-file water chains in narrow channels suggests strong interactions with external electric fields. The presence of electric fields is specifically expected to affect the equilibrium between the two orientations (up and down) of the water dipoles, and the equilibrium between the filled and empty state of the channel. In this paper we investigate both these aspects. We also determine the contribution of the energy and entropy to the free energy of filling and examine how they are altered by electric fields of varying magnitude.

The interior of a rigid carbon nanotube model is treated as a system in chemical and thermal equilibrium with a water bath. That allows us to describe the exchange of heat and particles rigorously in a grand-canonical ensemble and avoids the difficulties of separating a ''pore'' subsystem and a surrounding ''bath'' that are coupled through correlated fluctuations at the interface. The grand-canonical partition function can be evaluated term-by-term by using Metropolis Monte Carlo simulations[22] to extract the occupancy prob-

[a)]Current address: Institute for Physical Science and Technology, University of Maryland, College Park, Maryland 20742.
[b)]Electronic mail: rasaiah@maine.edu
[c)]Electronic mail: gerhard.hummer@nih.gov

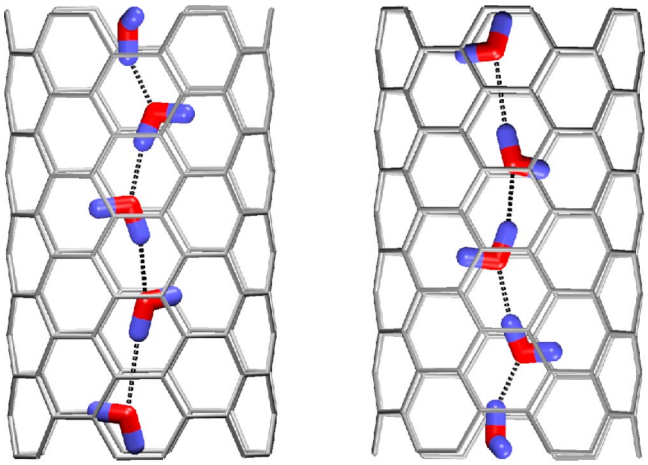

FIG. 1. Snapshots of the "up" (right) and "down" (left) states of the hydrogen-bonded water wires inside the nanotubes.

abilities as functions of the total chemical potential in the water bath and the external electric field inside the nanotube. Both periodically replicated[16] and finite tubes were studied. We are not concerned here with the mechanisms of how water molecules get in and out of the tube,[6,10,11] but instead focus on the thermodynamic and structural aspects of water within the tube. Such properties can be estimated by virtual transfer of water molecules between the finite or periodically replicated system and the bath, as in a grand-canonical ensemble. The analysis concentrates on the effects of homogeneous electric fields on the equilibria for filling and dipolar orientation and the effect of temperature on the thermodynamics of filling both in the absence and in the presence of electric fields. In particular, the difference in entropy and energy between water inside the tube and in the bulk fluid were determined from the temperature dependence of the occupancy probabilities.

The paper is outlined as follows: We first introduce the statistical-mechanical framework that will allow us to evaluate the terms in the grand-canonical partition function through Monte Carlo simulation and histogram analysis in the canonical ensemble. We then introduce a two-state model for the dipolar orientation of water, and analyze the effects of external electric fields on the water orientation and filling equilibria. To estimate the entropy and energy of confined water, we derive a relation between occupancy probabilities and the Helmholtz free energy of water in the nanotube. We then present details of the Monte Carlo simulations, followed by results for infinite and finite tubes in the presence and absence of electric fields, and as a function of temperature. We conclude by summarizing our results and highlighting possible implications in biomolecular systems, in particular the proton pump cytochrome *c* oxidase.[23]

II. THEORY

A. Occupancy fluctuations in the grand-canonical ensemble

Let us consider a system of fixed volume V that is in thermal and chemical equilibrium with a heat and particle bath. This system can be described in the grand-canonical ensemble at a given temperature T and total chemical potential μ. We note that heat and particle exchange between the bath and the system occur through an unspecified mechanism. The grand-canonical partition function is the generating function for the canonical ensemble. It is given by

$$\Xi=\sum_{N=0}^{\infty}\exp(N\beta\mu)Q(N,V,T)=\sum_{N=0}^{\infty}\frac{z^N}{N!}\int e^{-\beta U_N}d^N\mathbf{r}, \quad (1)$$

where the sum is over the number N of indistinguishable particles inside the volume V. The canonical partition function $Q(N,V,T)$ is related to the Helmholtz free energy through $A_N=-k_BT\ln Q(N,V,T)$. The integral in Eq. (1) is over the configurational coordinates (positions and orientations) of N particles. $z=q_1e^{\beta\mu}/V$ is the activity (with q_1 the one-particle partition function), and $\beta^{-1}=k_BT$ with k_B Boltzmann's constant. U_N is the classical configurational energy of the N-particle system. U_N can contain an external potential, e.g., the interaction with a container (such as a nanotube). The activity can also be expressed as

$$z=\rho e^{\beta\mu_{\mathrm{bulk}}^{\mathrm{ex}}}, \quad (2)$$

where $\mu_{\mathrm{bulk}}^{\mathrm{ex}}$ is the excess chemical potential of the reference bulk phase at density ρ and temperature T. The average number of particles is then given by

$$\langle N\rangle=\frac{\partial\ln\Xi}{\partial\ln z}=z\frac{\partial\ln\Xi}{\partial z}=\sum_{N=0}^{\infty}NP(N) \quad (3)$$

with $P(N)$ the probability of observing exactly N particles inside the volume V,

$$P(N)=\frac{z^N}{\Xi N!}\int e^{-\beta U_N}d^N\mathbf{r}. \quad (4)$$

By dividing probabilities, we obtain

$$\frac{P(N+1)}{P(N)}=\frac{z\int e^{-\beta U_{N+1}}d^{N+1}\mathbf{r}}{(N+1)\int e^{-\beta U_N}d^N\mathbf{r}}=\frac{zV}{N+1}\langle e^{-\beta(U_{N+1}-U_N)}\rangle_N. \quad (5)$$

The excess chemical potential μ_N^{ex} in the canonical ensemble (at fixed N, V, and T) satisfies

$$\exp(-\beta\mu_N^{\mathrm{ex}})=\langle\exp[-\beta(U_{N+1}-U_N)]\rangle_N, \quad (6)$$

as follows from Widom's test-particle insertion method.[24] Inserting this and the definition of z into Eq. (5), we have

$$\frac{P(N+1)}{P(N)}=\frac{\rho V}{N+1}e^{-\beta(\mu_N^{\mathrm{ex}}-\mu_{\mathrm{bulk}}^{\mathrm{ex}})}. \quad (7)$$

If μ_N^{ex} is identical to the excess chemical potential of the fluid in the bath, $\mu_{\mathrm{bulk}}^{\mathrm{ex}}$, then Eq. (7) leads to a Poisson distribution for $P(N)$ with mean $\langle N\rangle=\rho V$. Otherwise, the ratio $P(N+1)/P(N)$ can be determined, for instance, from Eq. (5) by test-particle insertion in the canonical ensemble of N particles. This requires the activity z as input, as given in Eq. (2), in terms of the bulk density ρ and the excess chemical potential $\mu_{\mathrm{bulk}}^{\mathrm{ex}}$ of the bulk fluid.

Alternatively, the average $\langle\cdots\rangle_N$ in Eqs. (5) and (6) can be determined by using Bennett's method of overlapping histograms.[25] The distribution of particle insertion energies ΔU in the system with N real particles is given by

$$p_{\mathrm{ins},N}(\Delta U)=\frac{\int e^{-\beta U_N}\delta(U_{N+1}-U_N-\Delta U)d^{N+1}\mathbf{r}}{\int e^{-\beta U_N}d^{N+1}\mathbf{r}}, \quad (8)$$

where $d^{N+1}\mathbf{r}$ denotes integration over the configuration space of particles 1 to N and the test particle. The distribution of particle removal energies ΔU from the system with $N+1$ real particles is given by

$$p_{\mathrm{rem},N+1}(\Delta U)=\frac{\int e^{-\beta U_{N+1}}\delta(U_{N+1}-U_N-\Delta U)d^{N+1}\mathbf{r}}{\int e^{-\beta U_{N+1}}d^{N+1}\mathbf{r}}. \quad (9)$$

By using the properties of Dirac's δ function, we obtain

$$\frac{p_{\mathrm{ins},N}(\Delta U)}{p_{\mathrm{rem},N+1}(\Delta U)}=e^{\beta\Delta U}\frac{\int e^{-\beta U_{N+1}}d^{N+1}\mathbf{r}}{V\int e^{-\beta U_N}d^N\mathbf{r}}=e^{\beta\Delta U}\langle e^{-\beta(U_{N+1}-U_N)}\rangle_N. \quad (10)$$

We can thus obtain the average $\langle\cdots\rangle_N$ from fitting $\ln[p_{\mathrm{ins},N}(\Delta U)/p_{\mathrm{rem},N+1}(\Delta U)]$ in the overlap region to a straight line with respect to ΔU.

To obtain the occupancy number distribution $P(N)$, we perform simulations in canonical ensembles of $N=1,2,...$ particles instead of using simulations with fluctuating particle numbers.[14,16] From the combination of these simulations, we estimate the average $\langle\cdots\rangle_N$ (either by test-particle insertion, or by the histogram method). By applying Eq. (5) successively, we construct the $P(N)$. $P(0)$ remains unspecified initially, but is obtained by normalization, $\Sigma_{N=0}^{\infty}P(N)=1$. It follows from Eq. (4) that $P(0)\equiv\Xi^{-1}$.

We note that by using Eq. (5), we can also express the average number of particles inside the observation volume V as a weighted sum of test-particle averages,

$$\langle N\rangle=\sum_{N=0}^{\infty}NP(N)=zV\sum_{N=0}^{\infty}P(N)\langle\exp[-\beta(U_{N+1}-U_N)]\rangle_N. \quad (11)$$

This relation was used in Ref. 4 to define the excess chemical potential $\mu_{\mathrm{NT}}^{\mathrm{ex}}$ of water in the volume V of the interior channel of a nanotube,

$$\exp(-\beta\mu_{\mathrm{NT}}^{\mathrm{ex}})=\sum_{N=0}^{\infty}P(N)\langle\exp[-\beta(U_{N+1}-U_N)]\rangle_N \quad (12)$$

such that $\langle N\rangle/\rho V=\exp[-\beta(\mu_{\mathrm{NT}}^{\mathrm{ex}}-\mu_{\mathrm{bulk}}^{\mathrm{ex}})]$. It follows from Eq. (12) that to obtain the proper $\mu_{\mathrm{NT}}^{\mathrm{ex}}$, test-particle insertion and removal have to be averaged over all occupancy states N of the volume V weighted with $P(N)$.

B. Temperature effects: entropy and energy of confined water

Entropy and energy differences of water inside the nanotube and in the bulk fluid can be estimated from the temperature dependence of the occupancy probabilities $P(N)$. To do this, we rewrite Eq. (4) as

$$P(N)=\frac{\exp(\beta\mu N-\beta A_N)}{\Xi}, \quad (13)$$

where A_N is the Helmholtz free energy of the system with N water molecules. Since $P(0)=\Xi^{-1}$, A_N can be determined from the ratio of probabilities in filled and empty states,

$$A_N=N\mu-k_{\mathrm{B}}T\ln\frac{P(N)}{P(0)}, \quad (14)$$

where we recall that μ is the total chemical potential of the bulk fluid. This allows us to extract the free energy difference, $\Delta A_N=A_N-A_{N,\mathrm{bulk}}$, of the confined molecules relative to those in the bulk fluid, and also the corresponding energy ΔU_N and entropy ΔS_N differences. Since $N\mu=A_{N,\mathrm{bulk}}+pV_{N,\mathrm{bulk}}$, it follows from Eq. (14) that

$$\Delta A_N=-k_{\mathrm{B}}T\ln\frac{P(N)}{P(0)}+pV_{N,\mathrm{bulk}}. \quad (15)$$

Here p is the pressure and $V_{N,\mathrm{bulk}}=N/\rho$ the volume of N molecules of the reference bulk fluid. The $pV_{N,\mathrm{bulk}}$ term per molecule is negligible ($\approx 1.8\times 10^{-3}$ kJ/mol) at ambient conditions and

$$\frac{\Delta A_N}{N}=-\frac{k_{\mathrm{B}}T}{N}\ln\frac{P(N)}{P(0)} \quad (16)$$

to high accuracy. But, $\Delta A_N=\Delta U_N-T\Delta S_N$, and it follows that

$$-\frac{1}{N}\ln\frac{P(N)}{P(0)}=\frac{\Delta U_N}{Nk_{\mathrm{B}}T}-\frac{\Delta S_N}{Nk_{\mathrm{B}}}, \quad (17)$$

where ΔU_N and ΔS_N refer to the energy and entropy difference between N water molecules in the nanotube and in bulk water. If for a given N and over a small temperature range, ΔU_N and ΔS_N are nearly constant, then it follows from Eq. (17) that a plot of $-N^{-1}\ln[P(N)/P(0)]$ vs T^{-1} furnishes $\Delta U_N/N$ and $\Delta S_N/N$ from the slope and y intercept, respectively. If ΔA_N is not linear in T^{-1}, then we can use

$$\Delta S_N=\frac{\partial}{\partial T}\left(k_{\mathrm{B}}T\ln\frac{P(N)}{P(0)}\right) \quad (18)$$

to obtain the entropy difference at a temperature T, again ignoring the temperature dependence of a small $pV_{N,\mathrm{bulk}}$ term.

C. Dependence on the electric field

We now consider an external electric field $\mathbf{E}$ and its effect on the occupancy numbers,

$$P(N;\mathbf{E})=\frac{z^N}{\Xi(\mathbf{E})N!}\int e^{-\beta(U_N-\mathbf{M}\cdot\mathbf{E})}d^N\mathbf{r} \quad (19)$$

where $\mathbf{M}=\Sigma_{i=1}^{N}\mathbf{m}_i$ is the total dipole moment vector of the N molecules with dipole moments $\mathbf{m}_i$. If the electric field acts also on the water bath,[26] then z will depend on $\mathbf{E}$. Here, we consider the field to act only on the water molecules in the nanotube, such that μ and z (for bulk water) are independent of $\mathbf{E}$.

For a completely filled tube ($N=N_0$) in the field-free case, the dipole moments are already almost fully aligned with the tube axis, $M_x \approx M_y \approx 0$ and $M_z \approx \pm \alpha N_0 m$. The scaling factor α is thus given by the amplitude of the total water dipole moment projected onto the tube axis, and can be estimated, e.g., from a field-free simulation, $\alpha \approx \langle |M_z|/(N_0 m)\rangle_{E_z=0}$ with $0 \ll \alpha \leqslant 1$. With this simplification we do not need to count over all possible orientations of individual water molecules in the tube. Instead, we can use a two-state description with an ''up'' state (energy $-\alpha N_0 m E_z$) and a ''down'' state (energy $\alpha N_0 m E_z$) for the dipole moment of the whole water array (Fig. 1). This ignores the presence of defects in the water dipole chain which are relevant, e.g., for the kinetics of reorientation.[19,21]

For a uniform field along the tube axis with $E_x=E_y=0$, the populations of the up and down states are approximately given by

$$p_u = \frac{e^{\beta\alpha N_0 m E_z}}{e^{\beta\alpha N_0 m E_z}+e^{-\beta\alpha N_0 m E_z}}, \tag{20}$$

$$p_d = \frac{e^{-\beta\alpha N_0 m E_z}}{e^{\beta\alpha N_0 m E_z}+e^{-\beta\alpha N_0 m E_z}}. \tag{21}$$

The average dipole moment is then given by

$$\langle M_z\rangle_{E_z} = \alpha N_0 m \tanh(\beta\alpha N_0 m E_z) \tag{22}$$

with variance

$$\langle M_z^2\rangle_{E_z} - \langle M_z\rangle_{E_z}^2 = (\alpha N_0 m)^2[1-\tanh^2(\beta\alpha N_0 m E_z)]. \tag{23}$$

Equation (22) predicts saturation at high fields. Similar saturation effects were studied earlier by Partenskii, Cai, and Jordan.[27]

For a narrow nanotube in water, we have found before[4,6] that it is either empty or filled with a well-defined number N_0 of water molecules, or it is fluctuating between empty and filled states. Within the two-state model for the dipolar orientation, the field-induced change in the ratio of filled to empty states is then given by

$$\frac{P(N_0;E_z)/P(N_0;0)}{P(0;E_z)/P(0;0)} = \cosh(\beta\alpha N_0 m E_z). \tag{24}$$

By taking the logarithm of Eq. (24), we obtain an expression for the difference between the transfer free energies of the filled tube at a field E_z along the z axis and at zero field,

$$\Delta A_{N_0}(E_z) - \Delta A_{N_0}(0) = -k_B T \ln\cosh(\beta\alpha N_0 m E_z), \tag{25}$$

which is an even function of the electric field E_z. At small fields, the free energy difference depends quadratically on the field E_z before it turns over to a linear decrease, with the dipoles saturated for $E_z \gtrsim (\beta\alpha N_0 m)^{-1}$.

TABLE I. Lennard-Jones parameters of the unmodified (Refs. 4 and 30) and modified (Ref. 4) carbon-water interactions.

	ϵ_{CO} (kcal/mol)	σ_{CO} (Å)
Unmodified	0.114 33	3.2752
Modified	0.064 61	3.4138

III. SIMULATIONS

To evaluate the grand-partition function, Eq. (1), we performed Monte Carlo simulations of water molecules in the canonical ensemble with different numbers of particles ($N=1$, 2, etc.) at temperatures of $T=280$, 290, 298, 310, and 320 K. The water molecules were confined to the interior of a rigid (6,6) ''armchair''-type carbon nanotube with a diameter (carbon-carbon) of 0.804 nm. Translational and rotational Monte Carlo moves were accepted according to the Metropolis criterion.[22] To enhance the sampling of dipolar orientations, an additional trial move consisted of a collective reorientation of the complete water chain by constructing the mirror image with respect to the $z=0$ plane. Two repeat lengths of the periodic tube, $L=1.453$ and 2.906 nm, were considered. Additional simulations were performed for ''closed'' tubes without periodic boundary conditions and with a hard potential precluding water oxygen atoms from moving beyond $z=\pm L/2$.

The effect of electric fields (0–1 V/nm) on nanotube filling was studied at 298 K, both for isolated tubes and under one-dimensional periodic boundary conditions. In addition, the periodically replicated tube was studied at 10 K intervals between 280 and 320 K at zero field and also at finite fields of 0.3333 and 1 V/nm. In the nonperiodic simulations, the electrostatic interactions were evaluated without a cutoff. In the periodic simulations, the length of the repeat unit in z direction was commensurate with the carbon geometry of the nanotube.

Water-water and water-carbon Lennard-Jones interactions were treated with the minimum-image approximation. Electrostatic interactions were evaluated using one-dimensional lattice sums corresponding to Ewald summation in three dimensions. Those sums can be conveniently approximated in terms of ψ functions.[21,28] By comparison with full evaluations of the slowly converging lattice sums, we found two terms in the expansion (up to $\psi^{(2)}$) to be sufficiently accurate.

During the simulations, we collected histograms of the particle-removal and particle-insertion energies, including the electrostatic self-interactions with the periodic images of the replicated system. Thermal equilibrium was established if the distributions of removal and insertion energies of states with $N+1$ and N water molecules, respectively, had sufficient overlap and satisfied Eq. (10). Typically, this required 10^7 Monte Carlo passes, in which each particle was attempted to be moved once. In some cases, the simulation length was increased by a factor of 5–10.

As in our earlier simulations,[4,6] the TIP3P model[29] was used to describe water. For the Lennard-Jones interactions of water with the carbon atoms of the nanotube we used ''unmodified'' AMBER parameters.[30] In addition, simulations

TABLE II. Excess chemical potential of TIP3P water as a function of temperature. Results for the pressure p and chemical potential μ^{ex}_{TIP3P} were obtained from simulations with 256 molecules in cubic boxes at constant number density ρ, as described in Ref. 4. In the chemical-potential calculations (Ref. 25), the Lennard-Jones interactions were evaluated up to a cutoff distance of half the box length, assuming a constant water density beyond for cutoff corrections. The electrostatic interactions were calculated by using a cubic-harmonic expansion for the Ewald interaction potential with coefficients given in Ref. 40. The last two columns list the experimental bulk water density and the excess chemical potential shifted according to Eq. (27), as used in the thermodynamics calculations.

T (K)	ρ (nm^{-3})	p (bar)	μ^{ex}_{TIP3P} (kJ/mol)	ρ_{exp} (nm^{-3})	Eq. (27) (kJ/mol)
290	33.2812	26	-25.7 ± 0.1	33.39	-25.7
300	32.9965	-8	-25.4 ± 0.1	33.31	-25.2
310	32.6125	-17	-25.0 ± 0.1	33.21	-24.7

with ''modified'' potentials corresponding to a reduced attractive interaction between carbon atoms and water (see Table I) were also performed.

The grand-canonical expressions for $P(N)$ require the total chemical potential of bulk water as input, or equivalently the excess chemical potential and the bulk density. For the bulk water phase, we use the experimental water particle density of 33.33 nm^{-3} (corresponding to a mass density of 997 kg/m^3) at 298 K, and an excess chemical potential $\mu^{ex}_{TIP3P}=-25.3$ kJ/mol estimated before[4] for TIP3P water at 300 K and a density of 987 kg/m^3 corresponding to 1 bar pressure.

In the studies of the temperature dependence, we use the experimental water density at atmospheric pressure.[31] To estimate the temperature-dependent excess chemical potential, we use the experimental water density and vapor pressure,[31] assuming an ideal gas in the vapor phase. For temperatures between 280 and 320 K, we obtain

$$\mu^{ex}_{bulk}(T)\approx\mu^{ex}_{bulk}(298\ \mathrm{K}) + 0.051\,36(T-298\ \mathrm{K})\ \mathrm{kJ/(mol\,K)} - 6.678\times10^{-5}(T-298\ \mathrm{K})^2\mathrm{kJ/(mol\,K^2)}. \quad (26)$$

The difference between the experimental excess chemical potentials at temperature T and 298 K was added to the excess chemical potential of bulk TIP3P water:

$$\mu^{ex}(T)\approx-25.3\ \mathrm{kJ/mol}+\mu^{ex}_{bulk}(T)-\mu^{ex}_{bulk}(298\ \mathrm{K}). \quad (27)$$

Together with the water density from experiment,[31] $\mu^{ex}(T)$ was used as a reference describing the bulk fluid in the calculations of temperature-dependent occupancy probabilities. We tested this with explicit simulations of TIP3P water at 290, 300, and 310 K, as summarized in Table II.

IV. RESULTS AND DISCUSSION

A. Infinite tubes without electric field

Figure 2 illustrates the histogram analysis used to evaluate the excess chemical potentials that enter into the grand-canonical partition function and the probability ratios $P(N+1)/P(N)$ given by Eq. (7). Results are shown for $N=0-5$ water molecules in the short nanotube (repeat length $L=1.453$ nm) at 298 K. Panel a (left) shows the histograms of energies for water insertion into a tube with one water molecule per repeat unit, and for removal from a tube with two water molecules. Also shown is the logarithm of the ratio of the insertion and removal probabilities together with a fit to a straight line of slope β. The negative intercept of the line with the $\Delta U=0$ axis is the excess chemical potential of water, $\beta\mu^{ex}_1$ (in units of k_BT), for a tube with $N=1$ water molecules. Panel b (right) shows the logarithm of the ratio of the insertion and removal probabilities for $N=0-5$ water molecules per repeat length.

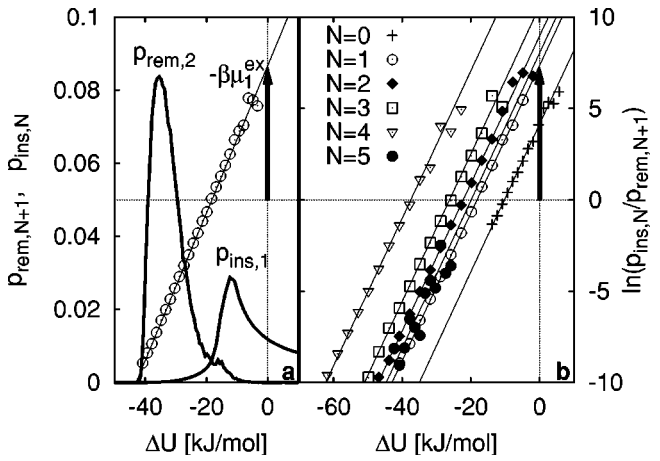

FIG. 2. Illustration of the histogram analysis for the short modified (i.e., less attractive) tube at $T=298$ K. Panel (a) on the left shows as thick lines the histograms of insertion and removal energies for $N=1$ and $N=2$, respectively, and the logarithm of their ratios (circles). The intercept of a straight-line fit with the $\Delta U=0$ axis gives the excess chemical potential, $-\beta\mu^{ex}_1$, as indicated by the vertical arrow. Panel (b) on the right shows the corresponding histogram analyses for N between 0 and 5.

Figure 3 shows the transfer free energy $\beta\Delta A_N=-\ln[P(N)/P(0)]$ for N water molecules at 298 K for tubes of repeat lengths $L=1.453$ and 2.906 nm, and for the unmodified and modified carbon-water Lennard-Jones interaction potentials. The $P(N)$ were calculated from Eq. (7) with the excess chemical potentials μ^{ex}_N determined from histogram analyses, as illustrated in Fig. 2.

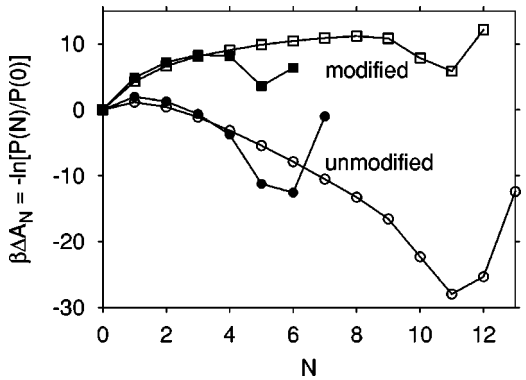

FIG. 3. Free energies of transfer ΔA_N in units of k_BT for short and long tubes with modified and unmodified carbon-water interactions, respectively, at 298 K.

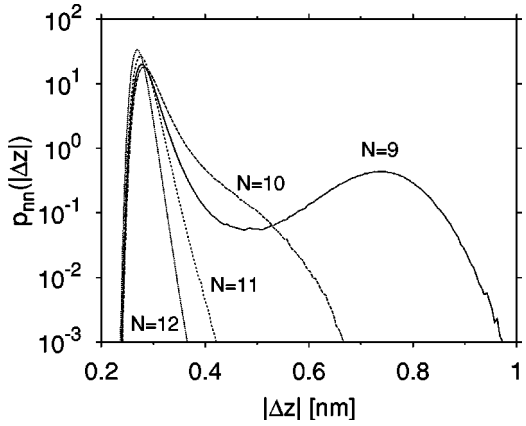

FIG. 4. Probability distributions of the distance $|\Delta z|$ along the tube axis between adjacent water-oxygen atoms for $N=9-12$ water molecules in the long unmodified tube (logarithmic scale) at 298 K.

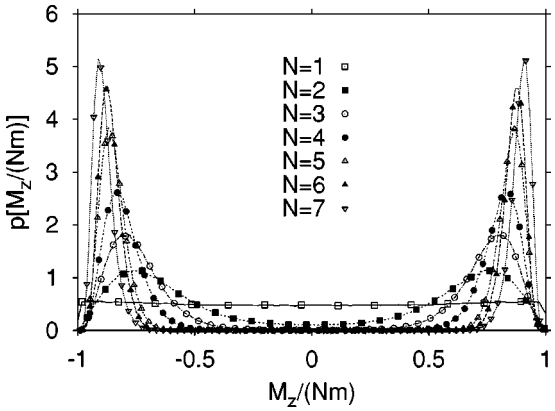

FIG. 5. Probability distribution of the total dipole moments of the water chains in the short tube with modified carbon-water interactions at 298 K in the absence of an external electric field. The total dipole moment is scaled by the number N and dipole moment m of water molecules. Results are shown for filling with $N=1-7$ water molecules.

At this temperature, tubes with unmodified carbon-water potentials are preferentially filled for both short and long tube repeat lengths. For short and long tubes filled with $N=6$ and 12 water molecules, we estimate free energies of $\approx -k_BT \ln[P(6)/P(0)] \approx -12.55k_BT$ and $-k_BT \ln[P(12)/P(0)] \approx -25.3k_BT$, respectively, or about $-2.1k_BT$ per water molecule independent of tube length. For $N=5$ and 10, the corresponding free energies are $-2.2k_BT$ per water molecule, again essentially independent of tube repeat length. However, compared to the short tube segment, water is more densely packed in the completely filled state of the long tube with $N=11$ molecules. The distribution of nearest-neighbor distances $|\Delta z|$ shown in Fig. 4 demonstrates that the long tube with $N=9$ water molecules has the chain predominantly ruptured, as indicated by a second peak near 0.75 nm. For $N=10$, the chain is stretched, as indicated by the enhanced shoulder near 0.4 nm distance, compared to the sharper peaks in the nearest-neighbor distributions for $N=9$, 11, and 12 water molecules. Similar behavior is seen for the probability distribution of water-oxygen atoms with respect to their distance from the tube axis (not shown). For $N=10$, the water molecules are found closer to the tube axis than for larger or smaller N, consistent with a ''stretched'' hydrogen-bond wire.

For the tubes with modified (i.e., less attractive) carbon-water interactions at 298 K, the empty states are more populated than the filled states, which appear in Fig. 3 as secondary minima at $N=5$ and 11, respectively. For short and long tubes filled with $N=5$ and 10 water molecules, respectively, we estimate free energies of $\approx -k_BT \ln[P(5)/P(0)] \approx 3.6k_BT$ and $-k_BT \ln[P(10)/P(0)] \approx 7.8k_BT$, respectively, or about $0.72k_BT$ and $0.78k_BT$ per water molecule. Compared to a finite tube solvated in water,[4,6] filling of the periodic tube is somewhat less favorable. For the solvated tube of length ~ 1.35 nm, with the same modified carbon-water interactions we estimated previously[4] that $-k_BT \ln[P(5)/P(0)] \approx 2.2k_BT$, i.e., more favorable for filling by about $0.3k_BT$ per water molecule than the periodic tube in equilibrium with the same bulk fluid.

Figure 5 displays the probability distributions at 298 K of the total water dipole moment (per water molecule and in units of the dipole moment of a single TIP3P water molecule) projected onto the tube axis. Results are shown for the short tube with modified carbon-water interactions, but are practically identical to those for the unmodified tube. In the absence of an external electric field, the distributions are symmetric and have two maxima near ± 1 corresponding to the two possible orientations of the hydrogen-bonded water chains formed along the tube axis. For $N=1$, the self-interaction with the periodic images leads to only a slight orientational preference compared to the constant value of an isotropic distribution. As the number N of water molecules increases, the distributions become sharper. For filled tubes (here, $N=5$), the dipole moments of the water molecules are almost fully aligned. As will be shown below, this leads to strong coupling to an external electric field along the tube axis that can be described accurately by a two-state model for the two water orientations.

B. Infinite tube with electric field

An external electric field parallel to the tube axis favors the filled state over the empty state. In Fig. 6, $\beta\Delta A_N = -\ln[P(N)/P(0)]$ is plotted as a function of the occupancy number N for electric fields of 0, 0.0333, 0.3333, and 1 V/nm for the short and long tubes, respectively, with modified (less attractive) carbon-water interactions. In the absence of the field, the empty state is preferred over the filled state (see Fig. 3). The total chemical potential μ and activity z of the bath water are assumed to be independent of the electric field which acts only on the water molecules in the tube. Figure 6 shows that a field of 0.033 33 V/nm has almost no effect on the filling. In contrast, at a field of 0.3333 V/nm, the filled and empty states occur with about equal probability $[\Delta A_N(N=11) \approx 0]$ for the long tube. At an even higher field of 1 V/nm, the filled state is strongly favored over the empty state for both the short and long tubes. We note that even though these are very large fields on a macroscopic length scale, one elementary charge in vacuum creates fields of 0.3333 and 0.0333 V/nm at distances of about 2 and 6.5 nm which are large on a molecular scale. Typical transmembrane

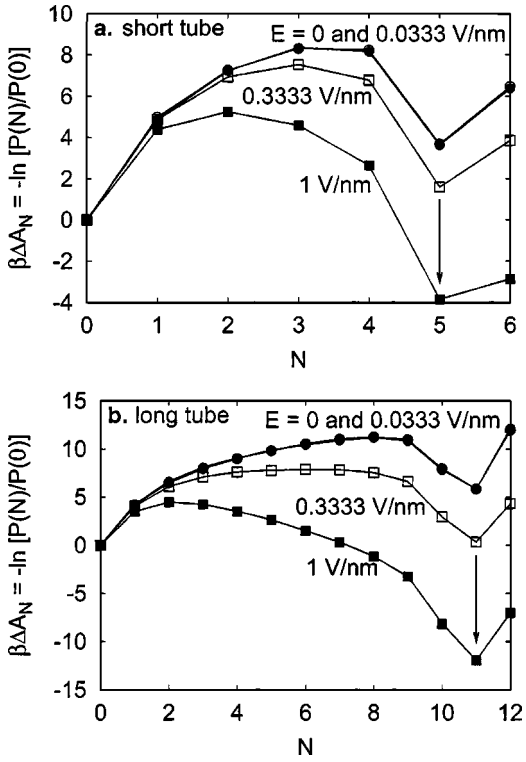

FIG. 6. Free energies of transfer ΔA_N in units of k_BT for (a) the short and (b) the long tube with modified carbon-water interactions at electric fields of 0, 0.0333, 0.3333, and 1 V/nm and $T=298$ K.

potentials in biological systems are in the range of 100–200 mV with corresponding averaged electric fields in the range of 0.02–0.06 V/nm.

Figure 7 compares the average and variance of the dipole moment of the water chain to the two-state model of Sec. II C. The parameter $\alpha=0.85$ of the two-state model was estimated independently from the average absolute total dipole moment in a short tube filled with $N_0=5$ water molecules, $\alpha=\langle|M_z|/(N_0m)\rangle$ at zero field. Data from simulations and the two-state model are in excellent agreement. The two-state model also accounts for the effects of electric fields

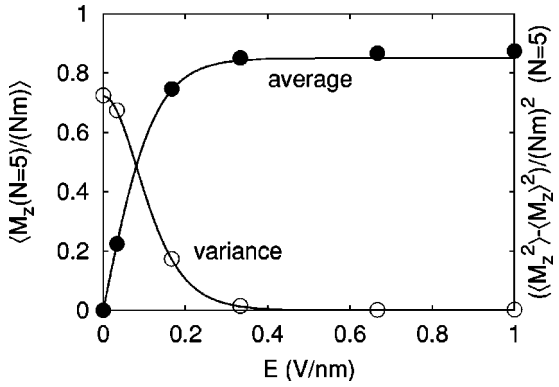

FIG. 7. Average (solid circles) and variance (open circles) of the total dipole moment (per water molecule and in units of the water dipole moment) as a function of the electric field parallel to the tube axis. Results are shown for a short tube segment (with modified carbon-water parameters) filled with $N=5$ water molecules. The solid lines are the results of Eqs. (22) and (23) for the two-state model.

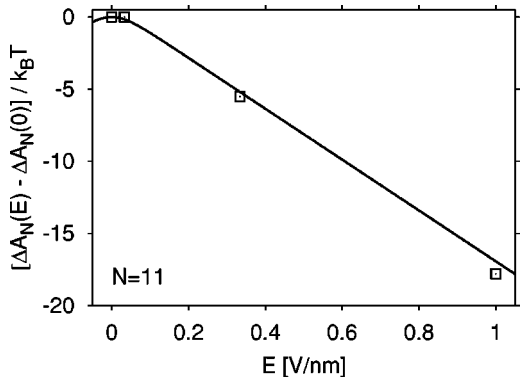

FIG. 8. Dependence of the transfer free energy on the electric field for the filled state ($N=11$) of the long modified tube at 298 K. The line is the result of the two-state model, Eq. (25).

on the equilibrium between empty and filled states (Fig. 8). Small deviations at high fields in Figs. 7 and 8 are caused by a small increase in the polarization of the water chain compared to the bounds $M_z=\pm\alpha Nm$ of the two-state model.

C. Finite tube

So far, we have only considered tubes formed by periodic replication of a tube segment along the tube axis. In such periodic tubes, an oriented water chain can interact favorably with its periodic image since the two dipole orientations are compatible. This mimics systems in which a hydrogen-bond donor is present at one end of the pore, and a hydrogen-bond acceptor at the other end. Periodicity is thus expected to favor the filled over the empty state. To investigate this, we have also performed calculations of finite tubes that were not periodically replicated. In those tubes, the water oxygen atoms were confined to a range of $0<z<1.453$ nm along the tube axis.

Figure 9 compares the filling behavior of closed finite tubes with and without electric field along the tube axis, and for unmodified and modified carbon-water interactions. We find that filling of closed (nonperiodic) tubes is indeed less favorable. For modified carbon-water interactions, the filled minimum is absent, even at an electric field of 0.3333 V/nm.

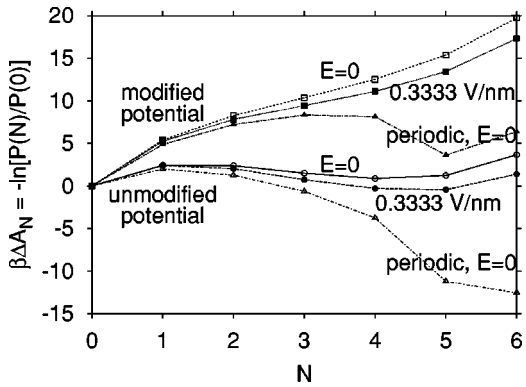

FIG. 9. Free energies of transfer ΔA_N in units of k_BT for the short tube at 298 K. Results are shown for finite (unlabeled) and periodically replicated tubes with modified and unmodified carbon-water Lennard-Jones potentials (Table I) in presence and absence of an electric field, respectively.

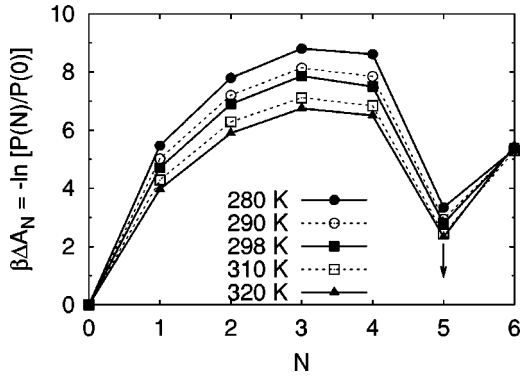

FIG. 10. Free energies of transfer as a function of N at different temperatures for the short, modified tube. Increasing the temperature lowers the free energy of the filled state ($N=5$).

For the unmodified carbon-water interactions, the filled minimum is shallower in the closed finite tube compared to the infinite periodic tube. This demonstrates the importance of interactions with the "solvent" at the openings of a finite tube, as included explicitly in the solvated tubes studied earlier[4,6] and in a lattice model system,[12] or here through interactions with the periodic images. Other important factors are the geometry and size of the pore.[32]

D. Entropy and energy of nanotube water

The grand-canonical formalism was used to study the temperature dependence of filling the short nanotube with water. In Fig. 10, $-\ln[P(N)/P(0)]$ is plotted against the occupancy number N for the short periodic tube with modified carbon-water interactions for temperatures between 280 and 320 K in the absence of an electric field. Remarkably, the filled state which corresponds to $N=5$ for the short modified tube, becomes increasingly populated as temperature goes up. The same behavior is also observed for the unmodified tube (data not shown).

To calculate the energy and entropy difference between nanotube and bulk water via Eq. (17), we plot $\Delta A_N/N = N^{-1}\ln P(N)/P(0)$ as a function of the inverse temperature. The plots [Fig. 11(a)] are linear for $N=1-6$ implying that ΔU_N and ΔS_N are essentially constant in this temperature range and can be determined from the slope and intercept, respectively. The temperature dependence of the occupancy probability $P(N)$ was also studied for the short tube with the modified potential at electric fields of 0.3333 and 1 V/nm. The plots of $N^{-1}\ln[P(N)/P(0)]$ vs T^{-1} are again linear [Fig. 11(b)].

Table III lists the energy ΔU_N and entropy ΔS_N contributions to the free energy of filling, $\Delta A_N=\Delta U_N-T\Delta S_N$, for the modified and unmodified nanotubes at a temperature of 298 K. The energy ΔU_N and entropy ΔS_N differences both favor filling of the short unmodified tube with $N=5$ in the temperature range 280–320 K. However, complete filling ($N=6$) corresponds to negative ΔU_N and negative ΔS_N, with the energy outweighing the contribution of the entropy to produce a favorable free energy of transfer. In contrast to this, the positive entropy difference ΔS_N for the modified short tube is too small to surmount the positive energy difference ΔU_N and lead to filling at zero field. The empty state is accordingly the preferred state at zero field.

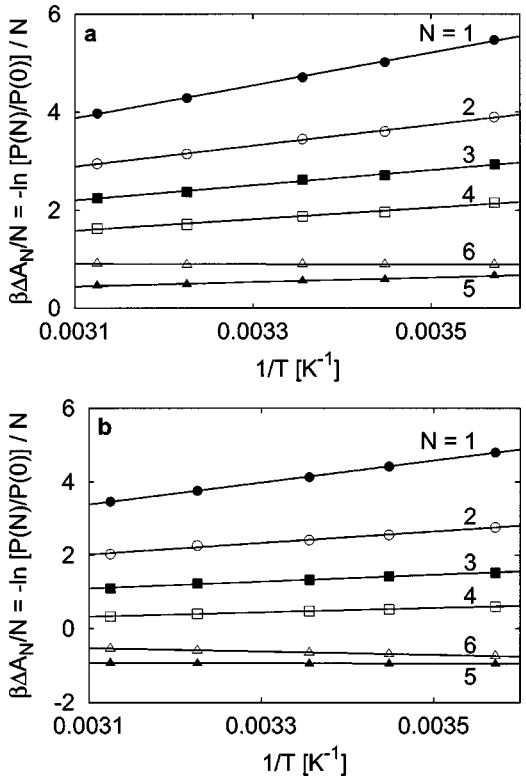

FIG. 11. Calculation of thermodynamic properties for filling the short modified tube using Eq. (17) at (a) $E=0.0$ V/nm and (b) $E=1.0$ V/nm. The slope is $\Delta U_N/Nk_B$ and the y intercept ($T^{-1}\to 0$) is $\Delta S_N/Nk_B$.

Figure 12 displays the calculated $\Delta U_N/N$ and $\Delta S_N/N$ as a function of N for the modified and unmodified short tubes at zero field and for the modified tube at fields of 0.3333 and 1 V/nm. Both the internal energy and entropy per particle are positive for the introduction of the first water molecule and then decrease with increasing occupancy number. As expected from first-order perturbation theory,[33] the difference in the internal energy per molecule for water molecules in the unmodified and modified tubes is almost independent of N (~ 7.5 kJ/mol), while the corresponding difference in entropies between these two tubes is small.

The internal energy ΔU_N can be broken up into the Lennard-Jones (LJ) interaction of water with the nanotube

TABLE III. Thermodynamic properties for the short nanotube in units of kJ/mol at zero field and $T=298$ K. ΔU_N, ΔS_N, and ΔA_N are differences in energy, entropy, and Helmholtz free energy, respectively, for N water molecules in the nanotube segment and in bulk water.

	Unmodified			Modified		
N	ΔU_N	$T\Delta S_N$	ΔA_N	ΔU_N	$T\Delta S_N$	ΔA_N
1	19.99	15.89	4.10	27.71	16.00	11.71
2	20.13	18.33	1.80	35.22	18.22	17.00
3	17.15	20.64	−3.49	38.38	19.10	19.28
4	9.58	21.29	−11.71	39.07	20.46	18.61
5	−15.55	15.07	−30.62	19.00	12.08	6.92
6	−42.36	−7.84	−34.52	−1.39	−14.70	13.31
7	−29.60	−25.32	−4.28			

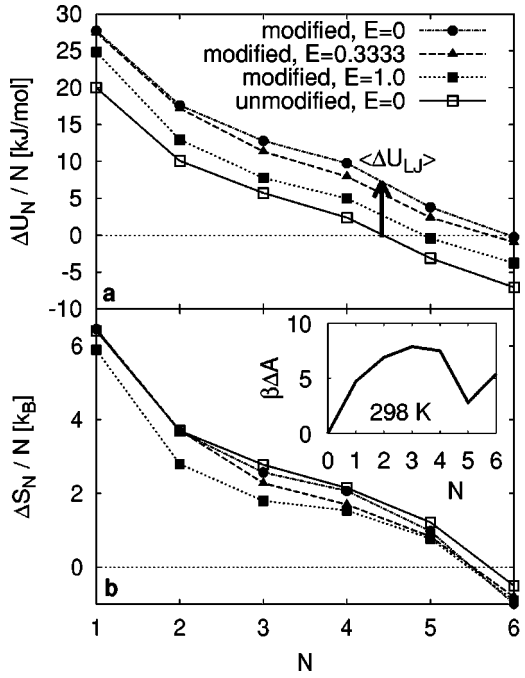

FIG. 12. Internal energy (top) and entropy (bottom) per molecule of water inside the short modified nanotube ($E=0$, 0.3333, and 1 V/nm) and the unmodified tube ($E=0$). The arrow in the top panel indicates the result of first-order perturbation theory (Ref. 33) $\langle \Delta U_{\mathrm{LJ}} \rangle = 7.5$ kJ/mol, for going from the unmodified to the modified LJ interactions. The inset in the bottom panel shows the transfer free energy $\beta \Delta A_N$ for the short modified nanotube at 298 K and $E=0$.

(NU_{LJ}), the hydrogen-bond interaction between water molecules [$(N-1)U_{\mathrm{HB}}$ and NU_{HB} for partially filled and filled tubes, respectively], and the energy for removing water from the bulk phase ($-NU_{\mathrm{bulk}}$). From the average LJ interaction of a single water molecule with the tube, we obtain $U_{\mathrm{LJ}} \approx -20$ and -12.5 kJ/mol for unmodified and modified tubes, respectively. For TIP3P water, $U_{\mathrm{bulk}} \approx -40$ kJ/mol. Together with a hydrogen bond energy $U_{\mathrm{HB}} \approx -23.5$ kJ/mol that is close to the binding energy of a water dimer,[31] this simple model reproduces the observed internal energies of transfer ΔU_N. This model also explains the difference in internal energies per molecule for water in modified and unmodified tubes, as shown in Fig. 12.

The large positive entropy for $N=1$ reflects the gain in free volume for a single water molecule inside the nanotube. The decrease in entropy per molecule with increasing N reflects a reduction in free volume, and an increase in the orientational and translational order as the tube is filled. Per hydrogen bond formed, the loss in entropy of about $50\ \mathrm{J\,mol^{-1}\,K^{-1}}$ is comparable in magnitude to that estimated for forming a water dimer (≈ 75–$110\ \mathrm{J\,mol^{-1}\,K^{-1}}$).[31]

The entropy difference $\Delta S_N/N$ between nanotube water and bulk water remains positive for $N \leqslant 5$ both for the modified and unmodified short nanotubes. At $N=5$ water molecules, the entropy differences are about $1.2k_{\mathrm{B}}$ and $1.0k_{\mathrm{B}}$ for unmodified and modified short tubes, respectively. That difference may partly be due to the larger free volume in the unmodified tube, but uncertainties in the calculated entropies are of comparable magnitude.

The positive relative entropy of $\sim 1k_{\mathrm{B}}$ per water molecule for the tube filled with $N=5$ molecules can be understood in part from the orientational freedom of the dangling hydrogen atom not involved in hydrogen bonding with the two neighboring water molecules (Fig. 1). This effect is not included in a lattice model of nanotube filling,[12] thus explaining why that model leads to emptying as temperature increases, even though it shows a reduction in the barrier between empty and filled states as is found here (Fig. 10). There are also contributions to the entropy from the collective rotation, translation, and rattling of water molecules in the hydrogen bonded chain for $N \leqslant 5$ in the short tube. However, we caution against overinterpreting the sign of the entropy of the filled state. In open tubes surrounded by water, for instance, the temperature dependence of the direct interactions between water molecules at the pore openings might affect the entropy of filling. Density fluctuations at the tube openings were found to be important for the filling kinetics in a lattice model.[12] More important than the sign is that water in one-dimensionally ordered chains can have entropies that are *comparable* to those of bulk water. The sensitivity to details is already apparent in the state with $N=6$ water molecules, for which the entropy of transfer becomes negative. In that compressed structure, water molecules are found to zig-zag about the tube axis, and the hydrogen bonds are nearly coplanar, resulting in a loss of rotational entropy (data for orientational distribution not shown). Changing the equation of state of the reference bulk phase further highlights the sensitivity of the entropy to details. From fits of the excess chemical potential and density of TIP3P water (Table II) to the temperature, we estimate that the entropy of TIP3P bulk water is larger by about $2k_{\mathrm{B}}$ per molecule than that obtained from Eq. (27) and the experimental bulk-water density. Using TIP3P water as a reference bulk fluid would thus make the $N=5$ state of the short tube entropically slightly *unfavorable*.

TABLE IV. Thermodynamic properties for the modified short nanotube in units of kJ/mol in the presence of a uniform electric field E parallel to the tube axis at $T=298$ K.

	$E=0.3333$ V/nm			$E=1.0$ V/nm		
N	ΔU_N	$T\Delta S_N$	ΔA_N	ΔU_N	$T\Delta S_N$	ΔA_N
1	27.48	15.99	11.49	24.85	14.58	10.27
2	34.38	18.37	16.01	25.87	13.89	11.98
3	34.02	16.94	17.08	23.31	13.39	9.92
4	31.83	16.88	14.95	19.93	15.22	4.71
5	12.00	10.22	1.78	−2.08	9.65	−11.73
6	−5.65	−12.47	6.82	−22.64	−12.96	−9.68

Table IV shows that moderate to large electric fields of 0.3333 and 1.0 V/nm have a larger effect on the energy difference ΔU_N than on the entropy difference ΔS_N, and the filled state of the short modified tube is favored over the empty state at a field $E=1.0$ V/nm. The loss in entropy of the filled state ($N=5$) with increasing field E is well explained by the two-state model for the orientation of the the water chain with a maximum loss of $k_{\mathrm{B}} \ln 2$. Finally we note that the filled and empty states have equal populations when $\Delta U_N = T\Delta S_N$ for $N=N_0$, the number of water molecules in the filled tube. This can be realized by changing the tempera-

ture or osmotic conditions, tuning the nanotube-water interaction, or applying an electric field.

V. CONCLUDING REMARKS

We have studied the occupancy and dipolar orientations of water in narrow hydrophobic pores as a function of the temperature and electric field acting on the water molecules. To confine the water we used carbon nanotubes, but similar results should be obtained for other pores of comparable geometry and low polarity. In the presence of electric fields, the dipolar equilibrium between the up and down states is shifted. Moreover, electric fields along the tube axis were shown to shift the equilibrium toward the filled state. The field dependence of the equilibrium properties of the filled states ($N=5$ for the short modified tube) is well described by a two-state model. Similar effects could be achieved by placing a dipole outside a finite carbon nanotube (data not shown).

From the effect of temperature on the occupancy probabilities, we determine the energy and entropy contributions to the free energy of filling carbon nanotubes. The entropy difference between water in the short nanotube and the bulk phase is positive, and thus favors filling, for all values of the occupancy number except $N=6$ which is the filled state of the unmodified tube. However, the exact value of the entropy of transfer depends on the reference bulk phase, and would become slightly negative for the filled state ($N=5$) at zero field if we used the temperature dependence of TIP3P water instead of the experimental equation of state. The energy difference ΔU_N for the filled tube ($N=6$ for the unmodified tube and $N=5$ for the modified tube) depends on the water-tube interaction, and is found to be negative for the unmodified tube (with relatively favorable water-tube interactions) and positive for the modified (less attractive) tube, as explained quantitatively by first-order perturbation theory with respect to the water-tube attractive interactions.[33] This leads to a global free energy minimum for the filled state ($N=6$) of the unmodified short nanotube. The local minimum that is observed in the free energy profile for the short modified tube at $N=5$ is entropic in origin, but is higher than the free energy of the empty tube, which is the preferred state at zero field. At high fields ($E=1.0$ V/nm) the decrease in the energy of the filled state is sufficient to make this the preferred state over the empty one.

Recent molecular dynamics simulations by Allen *et al.*[10,11] of water permeating through a nanopore connecting two reservoirs have been used to estimate energies and entropies of water in the pore and near its openings. While their pores had somewhat larger diameters and were connected directly to the water bath, a comparison with our results for narrow pores would nevertheless be instructive. However, their internal energies and entropies are only approximate, estimated without consideration of the correlated fluctuations at the interface of the pore and bath subsystems and the resulting ''solvent-reorganization'' contributions.[34] Nevertheless, because the filled state was favored at their conditions, and their approximate internal energies appear unfavorable for filling, one might conclude that the missing term in their entropies should be large and positive. Here, we indeed find positive (i.e., favorable) entropies of transfer up to the filled state of a periodically replicated single-file pore. However, definite conclusions for the larger pores of Allen, Hansen, and Melchionna[11] will require a more detailed thermodynamic analysis.

Our studies of a simple system have implications on the design of nanotube-based channels[35,36] and proton wires,[21] as well as on the functional mechanisms of biological water pores and proton pumps. The strong coupling between electric fields and the orientation of water molecules inside narrow nonpolar channels has been suggested as a key element in the proton-pump mechanism of cytochrome *c* oxidase.[23] That protein converts the energy released in the reduction of oxygen to water into an electrochemical potential in part by pumping protons across a membrane. In the mechanism of Wikström, Verkhovsky, and Hummer[23] for this vectorial transport of protons through the membrane, this is accomplished by orienting the water molecules in the weakly polar active site cavity by the electric field between the redox centers in such a way that ''pumping'' (through rapid proton transfer[21]) gates the electron transfer into the active site, and thus couples redox chemistry to the transfer of protons across the membrane against an electrochemical gradient. In addition to ordering the dipoles of confined water molecules, we also found here that electric fields can induce filling of previously empty nonpolar pores. Recent crystallographic studies of functional intermediates of the proteins cytochrome P450 (Ref. 37) and bacteriorhodopsin[38] suggest that such transient water filling can indeed be induced by the local electric fields caused by changes in the structure and ionization states of the proteins.[4,18,39]

ACKNOWLEDGMENTS

The authors thank Attila Szabo, Aparna Waghe, and Hao Yin for their help and discussions. S.V. gratefully acknowledges a predoctoral visiting fellowship from the NIDDK, National Institutes of Health. J.C.R. and S.V. acknowledge support from the National Science Foundation under Grant No. CHE9961336

[1] L. D. Gelb, K. E. Gubbins, R. Radhakrishnan, and M. Sliwinska-Bartkowiak, Rep. Prog. Phys. **62**, 1573 (1999).
[2] R. R. Meyer, J. Sloan, R. E. Dunin-Borkowski, A. I. Kirkland, M. C. Novotny, S. R. Bailey, J. L. Hutchison, and M. L. H. Green, Science **289**, 1324 (2000).
[3] M. Wilson and P. A. Madden, J. Am. Chem. Soc. **123**, 2101 (2001).
[4] G. Hummer, J. C. Rasaiah, and J. P. Noworyta, Nature (London) **414**, 188 (2001).
[5] T. Werder, J. H. Walther, R. L. Jaffe, T. Halicioglu, F. Noca, and P. Koumoutsakos, Nano Lett. **1**, 697 (2001).
[6] A. Waghe, J. C. Rasaiah, and G. Hummer, J. Chem. Phys. **117**, 10789 (2002).
[7] A. Wallqvist and B. J. Berne, J. Phys. Chem. **99**, 2893 (1995).
[8] X. Huang, C. J. Margulis, and B. J. Berne, Proc. Natl. Acad. Sci. U.S.A. **100**, 11953 (2003).
[9] O. Beckstein, P. C. Biggin, and M. S. P. Sansom, J. Phys. Chem. B **105**, 12902 (2001).
[10] R. Allen, S. Melchionna, and J. P. Hansen, Phys. Rev. Lett. **89**, 175502 (2002).
[11] R. Allen, J. P. Hansen, and S. Melchionna, J. Chem. Phys. **119**, 3905 (2003).
[12] L. Maibaum and D. Chandler, J. Phys. Chem. B **107**, 1189 (2003).

[13] X. Zhou, C.-Q. Li, and M. Iwamoto (submitted); cond-mat/0212381 at www.arxiv.org
[14] I. Brovchenko, D. Paschek, and A. Geiger, J. Chem. Phys. **113**, 5026 (2000).
[15] A. Wallqvist, E. Gallicchio, and R. M. Levy, J. Phys. Chem. B **105**, 6745 (2001).
[16] I. Brovchenko, A. Geiger, and A. Oleinikova, Phys. Chem. Chem. Phys. **3**, 1567 (2001).
[17] O. Beckstein and M. S. P. Sansom, Proc. Natl. Acad. Sci. U.S.A. **100**, 7063 (2003).
[18] G. Hummer, J. C. Rasaiah, and J. P. Noworyta, in *Technical Proceedings of the Second International Conference on Computational Nanoscience and Nanotechnology*, edited by M. Laudon and B. Romanowicz (Computational Publications, Cambridge, MA, 2002), pp. 124–127.
[19] R. Pomés and B. Roux, Biophys. J. **75**, 33 (1998).
[20] M. L. Brewer, U. W. Schmitt, and G. A. Voth, Biophys. J. **80**, 1691 (2001).
[21] C. Dellago, M. M. Naor, and G. Hummer, Phys. Rev. Lett. **90**, 105902 (2003).
[22] N. Metropolis, A. W. Rosenbluth, M. N. Rosenbluth, A. H. Teller, and E. Teller, J. Chem. Phys. **21**, 1087 (1953).
[23] M. Wikström, M. I. Verkhovsky, and G. Hummer, Biochim. Biophys. Acta **1604**, 61 (2003).
[24] B. Widom, J. Chem. Phys. **39**, 2808 (1963).
[25] C. H. Bennett, J. Comput. Phys. **22**, 245 (1976).
[26] J. C. Rasaiah, J. Chem. Phys. **77**, 5710 (1982).
[27] M. B. Partenskii, M. Cai, and P. C. Jordan, Chem. Phys. **153**, 125 (1991).
[28] G. Hummer (unpublished).
[29] W. L. Jorgensen, J. Chandrasekhar, J. D. Madura, R. W. Impey, and M. L. Klein, J. Chem. Phys. **79**, 926 (1983).
[30] W. D. Cornell, P. Cieplak, C. I. Bayley *et al.*, J. Am. Chem. Soc. **117**, 5179 (1995).
[31] G. S. Kell, in *Water. A Comprehensive Treatise*, edited by F. Franks (Plenum, New York, 1972), vol. 1, chap. 10, pp. 363–412.
[32] S. Vaitheeswaran, H. Yin, J. C. Rasaiah, and G. Hummer (unpublished).
[33] J. D. Weeks, D. Chandler, and H. C. Andersen, J. Chem. Phys. **54**, 5237 (1971).
[34] H. A. Yu and M. Karplus, J. Chem. Phys. **89**, 2366 (1988).
[35] F.-Q. Zhu and K. Schulten, Biophys. J. **85**, 236 (2003).
[36] A. Kalra, S. Garde, and G. Hummer, Proc. Natl. Acad. Sci. U.S.A. **100**, 10175 (2003).
[37] I. Schlichting, J. Berendzen, K. Chu *et al.*, Science **287**, 1615 (2000).
[38] B. Schobert, L. S. Brown, and J. K. Lanyi, J. Mol. Biol. **330**, 553 (2003).
[39] S. Taraphder and G. Hummer, J. Am. Chem. Soc. **125**, 3931 (2003).
[40] G. Hummer, L. R. Pratt, and A. E. García, J. Phys. Chem. **99**, 14188 (1995).